

AD-A036 613

CONTROL DATA CORP MELVILLE N Y TR6 DIV

NEAR FIELD PRESSURE FOR AN INFINITE PHASED ARRAY OF CIRCULAR PI--ETC(U)

F/G 17/1

JUN 66 V MANGULIS

NOBSR-93023

NL

UNCLASSIFIED

TR6-023-TN-66-18

1 OF 1  
AD  
A036613



ADA036613

61596

MOST Project - 4

WP22-1-42011

FRI 15 JUL 1966



CONTROL DATA  
CORPORATION



10 J. Mangulis

6

NEAR FIELD PRESSURE FOR AN INFINITE  
PHASED ARRAY OF CIRCULAR PISTONS

11

JUN 1966

12 41p.

SUBMITTED TO:

U. S. NAVY ELECTRONICS LABORATORY  
SAN DIEGO, CALIFORNIA

CONTRACT NO:

15

NObsr-93023

REPORT NO:

14

TRG-023-TN-66-18

DDC  
RECEIVED  
MAR 7 1977  
D

DISTRIBUTION STATEMENT A

Approved for public release  
Distribution Unlimited

6e<sup>7</sup>  
TRG/ A SUBSIDIARY OF CONTROL DATA CORPORATION  
ROUTE 110 • MELVILLE, NEW YORK 11749 • 516/531-0600

353 415

JB

ADDITIONAL FOR	
WFO	White Section <input checked="" type="checkbox"/>
DDO	Diff Section <input type="checkbox"/>
GRANDUNIONED	<input type="checkbox"/>
NOTIFICATION	
Per Hrs. on file	
BY	
DISTRIBUTION/AVAILABILITY CODES	
MAIL and/or SPECIAL	
A	

WP22-1-42011

NEAR FIELD PRESSURE FOR AN INFINITE  
PHASED ARRAY OF CIRCULAR PISTONS

V. Mangulis

Report No. 023-TN-66-18  
Contract NObsr-93023

Submitted to:

Navy Electronics Laboratory  
San Diego, Calif.

Approved:

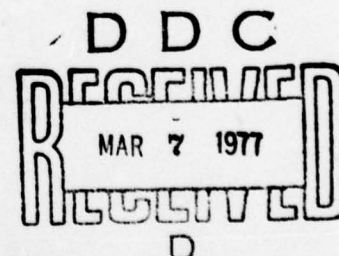
*Walton Graham*

Walton Graham,  
Department Head, TRG

Approved:

Marvin Baldwin,  
Project Technical Director, NEL

TRG, Incorporated  
A Subsidiary of Control Data Corporation  
Route 110  
Melville, N.Y.



June 1966

**DISTRIBUTION STATEMENT A**

Approved for public release;  
Distribution Unlimited







# TABLE OF CONTENTS

	Page
Abstract.....	iii
Acknowledgment.....	iv
List of Illustrations and Tables.....	v
A. INTRODUCTION.....	1
B. THE PRESSURE FIELD.....	2
C. RADIATION IMPEDANCE.....	14
D. CONCLUSIONS.....	17
References.....	20

## ABSTRACT



The near field pressure and the radiation impedance for an infinite phased array of circular pistons (with the same velocity magnitude) in a rigid plane baffle are calculated. A slowly convergent infinite series expression for the pressure, obtained from the appropriate Green's function, is transformed by the use of the Poisson's sum formula into a more rapidly convergent infinite series expression. Numerical results are presented. A rough estimate of the location and value of the maximum pressure in the near field is obtained under certain restrictions. The radiation impedance of a piston in the infinite array agrees well with the average radiation impedance of a piston in a large finite array.



ACKNOWLEDGMENT

This study was performed under contract NObsr-93023 with the Bureau of Ships. The opinions expressed are those of the author, and not necessarily those of the sponsoring agency.

The author wishes to thank J. Gobins who programmed the numerical calculations for a computer.

## LIST OF ILLUSTRATIONS AND TABLES

<u>Figure</u>	<u>Title</u>	<u>Page No.</u>
1	Part of the Infinite Array	23
2	$ P $ vs. $kz$ for several $ka$	24
3	$ P $ vs. $kx$ for several $\theta_0$	25
4	$ P $ vs. $kx$ for several $ka$	26
5	$ P $ vs. $kx$ for several $kd_1 = kd_2$	27
6	Pressure Contours in the Plane $z = 0$	28
7	Pressure Contours in the Plane $x = 0$	29
8	Pressure Contours in the Plane $y = 0$	30
9	$X$ vs. $kd_1 = kd_2$ for several $\theta_0$	31
10	$X$ vs. $ka$ for several $\theta_0$	32
11	$X$ vs. $\theta_0$ for several $ka$	33
12	Radiation Impedance vs. $\theta_0$ , Finite and Infinite Arrays	34

Table

1	Comparison of $ P_2 _{\max}$ and the actual Maximum of $ P $ .	22
---	--	----



## A. INTRODUCTION

A sonar designer is frequently faced with the task of calculating or estimating the peak pressure in the near field of a phased array because the usable power output of an acoustic underwater transducer is limited by the requirement that the acoustic pressure in water should not exceed the value at which cavitation begins. The computation of the peak pressure can be a rather formidable job because the summation of the pressures due to each array element usually cannot be reduced to anything simple analytically, and the location of the maximum pressure is not known a priori. Furthermore, to choose the optimum sonar design one would like to know how the pressure maximum changes when the sonar array parameters (size of elements, spacing between elements, number of elements, direction to which the array is steered in the far field, etc.) are varied, which might mean that the computation of the near field pressure has to be performed for a large number of arrays. Thus any simplifications are welcome as long as the simplifications permit to study the effects of some of the sonar parameters on the near field pressure.

Several calculations of the near field pressures for special distributions of elements in arrays are available.<sup>1-10</sup> For an infinite array two advantages in the representation of the near field pressure are attained:<sup>10</sup> 1) one has to consider the

pressure in front of one element only, because due to symmetry all elements are the same, except for a phase factor; 2) the infinite sum of pressures due to each array element can be transformed by the use of the Poisson's sum formula into a more rapidly convergent series of terms which resemble waveguide mode terms in the theory of electromagnetic waves.

One hopes that the inferences drawn from the infinite array calculations about the effects on the near field due to changes in the element sizes or spacings between elements will also apply to arrays with a finite number of elements. The two-dimensional problem of an infinite array of infinite vibrating strips in a rigid plane baffle has been studied before;<sup>10</sup> we will now consider the three-dimensional problem of an infinite phased array of circular pistons in a rigid plane baffle. The radiation impedances of the pistons will also be calculated. The velocity magnitudes of the pistons are assumed all to be equal, but the phases are adjusted so as to steer the far field pressure maximum in a specified direction.

## B. THE PRESSURE FIELD

Let the infinite array and baffle occupy the plane  $z = 0$ , (see Fig. 1). The piston centers are located at  $x = nd_1$ ,  $y = md_2$ ,  $n = 0, \pm 1, \pm 2, \dots$ ;  $m = 0, \pm 1, \pm 2, \dots$ . The velocity (in the  $z$ -direction) of the piston in the  $m^{\text{th}}$  row and  $n^{\text{th}}$  column is

assumed to be

$$v_{mn} = v e^{i\omega t + i\gamma_{mn}} \quad (1)$$

where  $v$  is a complex constant,  $\omega$  the radian frequency,  $t$  the time, and

$$\gamma_{mn} = -mkd_2' \sin\theta_0 \sin\phi_0 - nkd_1 \sin\theta_0 \cos\phi_0, \quad (2)$$

where  $k = \omega/c$ ,  $c$  is the velocity of sound in water, and  $\theta_0$ ,  $\phi_0$  are angles in spherical coordinates which determine the direction to which the far field pressure maximum is steered.

If the actual pressure at the observation point due to the  $m^{\text{th}}$ ,  $n^{\text{th}}$  piston alone is  $p_{mn}$ , let  $P_{mn}$  be a dimensionless pressure,

$$P_{mn} = p_{mn} / \rho c v e^{i\omega t}, \quad (3)$$

where  $\rho$  is the density of water. Similarly let  $P$  be the total dimensionless pressure at the observation point due to all pistons,

$$P = \sum_{m=-\infty}^{\infty} \sum_{n=-\infty}^{\infty} P_{mn} e^{i\gamma_{mn}} \quad (4)$$

By the use of a Green's function  $P_{mn}$  can be written as<sup>11,12</sup>

$$P_{mn} = (ik/2\pi) \int_0^{2\pi} d\alpha_0 \int_0^a dr_0 r_0 e^{-ikR_{mn}}/R_{mn} \quad (5)$$

where  $R_{mn}$  is the distance from a point on the  $m^{\text{th}}$ ,  $n^{\text{th}}$  piston at  $r_0$ ,  $\alpha_0$  to the observation point at  $x$ ,  $y$ ,  $z$ ; see Fig. 1;

$$R_{mn} = (x_n^2 + y_m^2 + z^2)^{1/2}, \quad (6)$$

$$x_n = x - nd_1 - r_0 \cos \alpha_0, \quad (7)$$

$$y_m = y - md_2 - r_0 \sin \alpha_0. \quad (8)$$

We now use the following integral representation for spherical waves<sup>13</sup>

$$\frac{e^{-ikR_{mn}}}{R_{mn}} = \frac{1}{2\pi^2} \int_{-\infty}^{\infty} ds_1 \int_{-\infty}^{\infty} ds_2 \int_{-\infty}^{\infty} ds_3 \frac{e^{-is_1 x_n - is_2 y_m - is_3 z}}{s_1^2 + s_2^2 + s_3^2 - k^2} \quad (9)$$

which, when integrated over  $s_3$ , becomes



$$\frac{e^{-ikR_{mn}}}{R_{mn}} = \frac{1}{2\pi} \int_{-\infty}^{\infty} ds_1 \int_{-\infty}^{\infty} ds_2 \frac{e^{-is_1 x_n - is_2 y_m - qz}}{q} \quad (10)$$

where

$$q = \begin{cases} i(k^2 - s_1^2 - s_2^2)^{1/2}, & 0 \leq s_1^2 + s_2^2 \leq k^2, \\ (s_1^2 + s_2^2 - k^2)^{1/2}, & s_1^2 + s_2^2 > k^2. \end{cases} \quad (11)$$

If we combine Eqs. (4), (5), and (10), and interchange summation and integration, we obtain

$$P = \frac{ik}{(2\pi)^2} \int_0^{2\pi} d\alpha_0 \int_0^a dr_0 r_0 \sum_{m=-\infty}^{\infty} \sum_{n=-\infty}^{\infty} \int_{-\infty}^{\infty} ds_1 \int_{-\infty}^{\infty} ds_2 \quad (1/q) \exp(i\gamma_{mn} - is_1 x_n - is_2 y_m - qz) \quad (12)$$

We now apply Poisson's sum formula<sup>14,15</sup>

$$\sum_{n=-\infty}^{\infty} \int_{-\infty}^{\infty} ds f(s) e^{2\pi i ns} = \sum_{n=-\infty}^{\infty} f(n) \quad (13)$$

twice to Eqs. (12), which yields

$$P = \frac{i}{d_1 d_2} \sum_{n=-\infty}^{\infty} \sum_{m=-\infty}^{\infty} \frac{e^{-T(n,m)kz}}{T(n,m)} \int_0^{2\pi} d\alpha_0 \int_0^a dr_0 r_0 \exp \left[ i h(n) (kr_0 \cos \alpha_0 - kx) + i g(m) (kr_0 \sin \alpha_0 - ky) \right]. \quad (14)$$

$$h(n) = \sin \theta_0 \cos \theta + 2\pi n / kd_1 \quad (15)$$

$$g(m) = \sin \theta_0 \sin \theta + 2\pi m / kd_2 \quad (16)$$

$$w(n,m) = \left\{ [h(n)]^2 + [g(m)]^2 \right\}^{1/2} \quad (17)$$

$$T(n,m) = \begin{cases} i \left\{ 1 - [w(n,m)]^2 \right\}^{1/2}, & 0 \leq w(n,m) \leq 1; \\ \left\{ [w(n,m)]^2 - 1 \right\}^{1/2}, & w(n,m) > 1. \end{cases} \quad (18)$$

Since<sup>16</sup>

$$\begin{aligned} & \int_0^{2\pi} d\alpha_0 \exp \left\{ i k r_0 [h(n) \cos \alpha_0 + g(m) \sin \alpha_0] \right\} \\ &= 2\pi J_0 [w(n,m) k r_0], \end{aligned} \quad (19)$$

where  $J_0$  is a Bessel function of order zero, and since<sup>17</sup>

$$\int_0^a dr_0 r_0 J_0(wkr_0) = (a/wk) J_1(wka) \quad (20)$$

where  $J_1$  is a Bessel function of order one, we finally obtain from Eq. (14)

$$P = \frac{i\pi a^2}{d_1 d_2} \sum_{n=-\infty}^{\infty} \sum_{m=-\infty}^{\infty} \frac{2J_1[w(n,m)ka]}{w(n,m)ka} \cdot \frac{e^{-ih(n)kx - ig(m)ky - T(n,m)kz}}{T(n,m)} \quad (21)$$

which is the desired exact expression for the pressure at  $x, y, z$  (either near field or far field) due to the infinite array.

The form of Eq. (21) is similar to the expansions of electromagnetic fields in waveguide modes.<sup>18</sup> The double series in Eq. (21) is more rapidly convergent than the original series from Eqs. (4) and (5); for  $z > 0$  the terms in the sum are decreasing exponentially with increasing  $m$  and  $n$ , and for  $z = 0$  the terms are decreasing as  $[(n/d_1)^2 + (m/d_2)^2]^{5/4}$ .

Let us now consider some special cases of Eq. (21). If  $kz \gg 1$  and  $kd_1 < \pi$ ,  $kd_2 < \pi$ , all the terms are exponentially decreasing except the one for  $n = m = 0$ . Since

$$w(0,0) = \sin\theta_0 \quad (22)$$

and

$$T(0,0) = i \cos \theta_0, \quad (23)$$

if we neglect the exponentially attenuated terms, we obtain a single-term approximation for the pressure

$$P \approx P_1 = \frac{\pi a^2}{d_1 d_2} \cdot \frac{2J_1(k \sin \theta_0)}{k \sin \theta_0} \cdot P_c, \quad kz \gg 1, \quad (24)$$

where  $P_c$  is the dimensionless pressure which one would have in the water if the whole  $z = 0$  plane were vibrating continuously with the normal velocity

$$v_c = v e^{i\omega t - ikx \sin \theta_0 \cos \theta_0 - iky \sin \theta_0 \sin \theta_0}; \quad (25)$$

i.e., if instead of a plane partially filled with pistons (each of which move with the same velocity as a rigid body) we would have a plane on which each infinitesimal area element moves with the velocity given by Eq. (25), then the pressure would be<sup>10</sup>

$$P_c = (1/\cos \theta_0) \exp(-ikx \sin \theta_0 \cos \theta_0 - iky \sin \theta_0 \sin \theta_0 - ikz \cos \theta_0) \quad (26)$$



Thus the approximate  $P_1$  as compared to  $P_c$  for  $kz \gg 1$  is reduced by the ratio of the piston area  $\pi a^2$  to the area of the array per piston  $d_1 d_2$  (because only the fraction  $\pi a^2 / d_1 d_2$  of the plane  $z = 0$  is vibrating in the piston array, while the whole plane is vibrating for the continuous plane radiator) and by the directivity of the circular piston  $2J_1(k a \sin \theta_0) / (k a \sin \theta_0) \leq 1$  (because the piston vibrates as a rigid body, therefore in a direction  $\theta_0 \neq 0$  the wavelets arriving from different portions of the same piston are not quite in phase, which results in partial cancellation; all the waves are in phase for the continuous plane radiator).

The  $n = m = 0$  term dominates, and we obtain  $P_1$  from Eq. (24) as an approximation for  $P$  also when  $d_1 \rightarrow 0$ ,  $d_2 \rightarrow 0$ ,  $a \rightarrow 0$ , i.e., when the piston array consists of small pistons close together, because such an array approximates the continuous plane radiator.

Fig. 2 shows  $|P|$  vs.  $kz$  for equal spacings between rows and columns,  $kd_1 = kd_2 = 3$ , and three values of the piston radii,  $ka = 0.5, 1.0$ , and  $1.5$ ; the pressure is evaluated on the axis through the center of a piston,  $kx = ky = 0$ , and the array radiates in the broadside direction normal to the plane containing the array,  $\theta_0 = \phi_0 = 0^\circ$ . For  $ka = 1.5$  the pistons are touching each other. For large values of  $kz$   $|P|$  approaches the constant  $|P_1|$  given by Eq. (24).

Fig. 3 shows  $|P|$  vs.  $kx$  for  $\theta_0 = 0^\circ, 60^\circ$ , and  $80^\circ$ , and  $\phi_0 = 0^\circ$ ; the other parameters are:  $kd_1 = kd_2 = 3$ ,  $ka = 1$ ,  $ky = kz = 0$ . For  $\theta_0 = 0^\circ$  the pressure distribution is relatively smooth, while for larger angles it becomes more undulatory. As  $\theta_0$  increases, the maximum  $|P|$  increases because the leading  $n = m = 0$  term in Eq. (21) is proportional to  $1/T(0,0) = 1/\cos\theta_0$ . For  $\theta_0 \rightarrow 90^\circ$  we would have  $|P| \rightarrow \infty$ .

The single-term approximation  $P_1$  does not show any undulatory behavior; therefore let us obtain a two-term approximation  $P_2$  to explain the maxima and minima in Fig. 3. For simplicity let  $\phi_0 = 0^\circ$ ,  $kd_1 < \pi$ ,  $kd_2 \leq kd_1$ , and  $\theta_0 > 0^\circ$ , then the next largest term after the  $n = m = 0$  term is the  $n=-1, m=0$  term. Let us call the approximation consisting of the two terms  $n=-1, 0$  and  $m=0$  the pressure  $P_2$ . Let us further assume that  $ka$  is small enough so that  $2J_1[w(n,m)ka]/w(n,m)ka \approx 1$  for both terms. Thus we obtain an approximation which for  $\phi_0 = 0^\circ$  is independent of the  $y$ -coordinate:

$$P_2 = \frac{\pi a^2}{d_1 d_2} e^{-ikx \sin \theta_0} \left\{ \frac{e^{-ikz \cos \theta_0}}{\cos \theta_0} + \frac{ie^{i2\pi(x/d_1) - kz} \left\{ [(2\pi/kd_1) - \sin \theta_0]^2 - 1 \right\}^{1/2}}{\left\{ [(2\pi/kd_1) - \sin \theta_0]^2 - 1 \right\}^{1/2}} \right\} \quad (27)$$

Consider the case  $kz = 0$ , then

$$|P_2| = \frac{\pi a^2}{d_1 d_2} \left| \frac{1}{\cos \theta_o} + \frac{e^{i[2\pi(x/d_1) + \pi/2]}}{\left\{ \left[ (2\pi/kd_1) - \sin \theta_o \right]^2 - 1 \right\}^{1/2}} \right| \quad (28)$$

The two terms in Eq. (28) can be considered as vectors in the complex plane. Thus we will have a maximum when the phase  $2\pi(x/d_1) + \pi/2$  of the second term becomes zero, or when the x-coordinate is

$$x_{\max} = -d_1/4, \quad (29)$$

independent of  $\theta_o$ ,  $d_2$ , or  $a$ .

Similarly a minimum will be obtained at

$$x_{\min} = +d_1/4. \quad (30)$$

The positions of the minima and the maxima agree well with the data in Fig. 3 for  $\theta_o > 0^\circ$ . For the values at the maximum and at the minimum Eq. (28) yields 1.19 and 0.21 at  $\theta = 60^\circ$ ; and 2.74 and 1.29 at  $\theta = 80^\circ$ , which are in a reasonable agreement with the values shown in Fig. 3.

Eq. (28) yields the maximum pressure

$$|P_2|_{\max} = \frac{\pi a^2}{d_1 d_2} \left\{ \frac{1}{\cos \theta_0} + \frac{1}{\left\{ \left[ (2\pi/kd_1) - \sin \theta_0 \right]^2 - 1 \right\}^{1/2}} \right\} \quad (31)$$

under the condition  $kz = 0$ . However, for  $kz > 0$  the second term in the more general Eq. (27) is exponentially decreased; therefore, even if we consider all values of  $x, y$ , and  $z$ , the absolute maximum of  $|P_2|$  must be on the plane  $kz = 0$ , and its value is given by Eq. (31), when  $\phi_0 = 0^\circ$ ,  $\theta_0 > 0^\circ$ ,  $kd_1 < \pi$ , and  $kd_2 \leq kd_1$ .

Fig. 4 shows  $|P|$  vs.  $kx$  for  $ka = 0.5, 1.0$ , and  $1.5$ , and  $kd_1 = kd_2 = 3$ ,  $ky = kz = 0$ ,  $\phi_0 = 0^\circ$ ,  $\theta_0 = 60^\circ$ . The pressure levels increase as  $ka$  increases because a larger fraction of the array plane radiates. A larger fraction of the array plane radiates also if  $ka$  is kept constant and  $kd_1$  and  $kd_2$  are decreased.  $|P|$  vs.  $kx$  for the latter case is shown in Fig. 5, where  $ka = 1$ ,  $kd_1 = kd_2 = 2, 2.5$ , and  $3$ , and  $kz = ky = 0$ ,  $\phi_0 = 0^\circ$ ,  $\theta_0 = 60^\circ$ . Note that for  $kd_1 = kd_2 < 3$  in Fig. 5 more than one cycle in the undulatory pressure is shown, because due to symmetry the pressure values are repeated at  $x, x \pm d_1, x \pm 2d_1$ , etc. The pressure distribution becomes relatively more undulatory as the spacing between pistons is increased. When  $ka = 1.5$  and  $kd_1 = kd_2 = 3$  in Fig. 4, and when  $ka = 1$  and  $kd_1 = kd_2 = 2$  in Fig. 5, then the pistons are touching each other, and the same fraction  $\pi/4$  of the array plane radiates in both cases. However, the maximum pressure in Fig. 4 for the larger piston  $ka = 1.5$  is about 24% larger than for the smaller piston  $ka = 1$  in Fig. 5.



The pressure is also more undulatory (i.e., the ratio of the maximum pressure to the minimum pressure increases) for the larger piston. All of the above features can be explained qualitatively by considering the two-term approximation  $P_2$ . As  $kd_1$  is increased, the magnitude of the second term in the parentheses in  $P_2$  in Eq. (28) is increased; therefore the pressure becomes more undulatory as the spacing between pistons is increased. If we keep the ratio  $\pi a^2/d_1 d_2$  constant in Eq. (28) or Eq. (31), then for a larger piston we have a larger  $kd_1$ , and thus a larger maximum pressure and a more undulatory pressure distribution.

Although  $P_2$  is useful as a guide to the general behavior of the pressure, it is of less value in the calculation of the actual pressure magnitudes; see Table I. Furthermore,  $P_2$  does not agree with the behavior of the pressure for  $ka = 0.5$  in Fig. 4; while the maxima and minima should be located at  $\pm d_1/4$  independent of  $\theta_0$ ,  $d_2$ , or  $a$ , the maxima and minima have been shifted for the  $ka = 0.5$  curve in Fig. 4. This curve is the only one of those shown in Figs. 3, 4, and 5, for which  $a < d_1/4$ , i.e., for which Eq. (29) predicts a maximum pressure on the adjacent baffle off the surface of the piston; however, the actual maximum is on the surface of the piston.

Moreover, according to Eq. (27)  $P_2$  is independent of  $ky$ , while the contours of  $|P|$  in Fig. 6 for  $z = 0$  show a  $ky$  dependence. The pressure contours in the planes  $x = 0$  and  $y = 0$  are shown in Figs. 7 and 8, when  $kd_1 = kd_2 = 3$ ,  $ka = 1$ ,  $\theta_0 = 0^\circ$ ,

and  $\theta_0 = 60^\circ$ . Since  $\phi_0 = 0^\circ$ , the pressure field is symmetric about the x-axis, and only pressures for  $ky \geq 0$  are shown. For large values of  $kz$ ,  $|P| = 0.63$  in Figs. 7 and 8.

### C. RADIATION IMPEDANCE

The force on the  $m^{\text{th}}, n^{\text{th}}$  piston divided by the velocity  $v_{mn}$ , is the radiation impedance  $\rho c \pi a^2 Z$ , where  $Z$  is a dimensionless radiation impedance coefficient. Due to symmetry  $Z$  is the same for all pistons.

$$Z = (1/\pi a^2) \int_0^{2\pi} d\alpha \int_0^a dr \, r P \Big|_{z=0} = R + iX \quad (32)$$

where  $x = r \cos \alpha$ ,  $y = r \sin \alpha$ , and  $P$  is given by Eq. (21). The integrals in Eq. (32) are the same as in Eqs. (19) and (20), thus

$$Z = \frac{i\pi a^2}{d_1 d_2} \sum_{n=-\infty}^{\infty} \sum_{m=-\infty}^{\infty} \left\{ \frac{2J_1(w(n,m)ka)}{w(n,m)ka} \right\}^2 \frac{1}{T(n,m)} \quad (33)$$

For  $kd_1 < \pi$ ,  $kd_2 < \pi$  the dimensionless radiation resistance  $R$  is given by the  $n = m = 0$  term,

$$R = \frac{\pi a^2}{d_1 d_2} \left[ \frac{2J_1(ka \sin \theta_0)}{ka \sin \theta_0} \right]^2 \frac{1}{\cos \theta_0}, \quad (34)$$

while the reactance  $X$  is given by the infinite sum without the  $n = m = 0$  term. The corresponding quantities  $Z_c = R_c + iX_c$  for the continuous plane radiator are<sup>10</sup>

$$R_c = 1/\cos\theta_0, \quad (35)$$

$$X_c = 0. \quad (36)$$

The fact that the radiation resistance should be proportional to  $1/\cos\theta_0$  can also be deduced for a finite array for  $\theta_0 < \pi/2$  by the use of arguments involving the array beamwidth in the far field.<sup>8</sup>

One could also obtain the radiation impedance by summing an infinite series of the appropriate mutual coupling coefficients<sup>19</sup>; however, the series in Eq. (33) converges more rapidly than such a series of mutual coupling coefficients, and thus is more useful. An approximate expression for  $Z$  has been obtained before<sup>20</sup> by the application of Poisson's sum formula to a summation of approximate mutual coupling coefficients, but the exact Eq. (33) is even simpler than the approximate expression.

Fig. 9 shows  $X$  vs.  $kd_1 = kd_2$  for three values of  $\theta_0$ , and  $ka = 0.5$ ,  $\theta_0 = 0^\circ$ . As the spacing between pistons is increased, the radiation resistance  $R$  is decreased, which is obvious from Eq. (34), and the radiation reactance  $X$  is increased,

as shown in Fig. 9. The radiation resistance is proportional to the energy which is radiated to the far field; the radiation reactance is proportional to the energy which just fluctuates in the near field.<sup>21</sup> When the whole plane is vibrating, then there is no energy fluctuating in the near field, see Eq. (36), while for the set of parameters used in Fig. 9 the near field fluctuating energy is increased as the ratio of the active piston areas to the passive baffle area is decreased by increasing  $kd_1 = kd_2$  and keeping  $ka$  constant.

If the ratio of the active piston areas to the passive baffle area is decreased by decreasing  $ka$  and keeping  $kd_1 = kd_2$  constant, the near field fluctuating energy may be increased or decreased, see Fig. 10, where  $X$  vs.  $ka$  is shown for three values of  $\theta_0$ , and  $kd_1 = kd_2 = 3$ ,  $\phi_0 = 0^\circ$ .

Fig. 11 shows  $X$  vs.  $\theta_0$  for three values of  $ka$ , and  $kd_1 = kd_2 = 3$ ,  $\phi_0 = 0^\circ$ .

In Fig. 12 the radiation impedance of a piston in the infinite array is compared with the average radiation impedance  $R_{av} + iX_{av}$  of a piston in a finite array of 12 rows (parallel to the  $y$ -axis) and 229 columns (parallel to the  $x$ -axis). The radiation impedance of a piston in the finite array is obtained by summing the appropriate mutual coupling coefficients,<sup>19</sup> and in general the impedances vary from piston to piston. The average radiation impedance for the finite array is obtained



by summing the impedances of all the pistons and by dividing the sum by the total number of pistons. The agreement in Fig. 12 for  $kd_1 = kd_2 = 2.51$ ,  $ka = 0.80$ ,  $\phi_0 = 0^\circ$ , is good except near  $\theta_0 = 90^\circ$  where, of course,  $R$  for the infinite array becomes infinite, while for the finite array  $R_{av}$  is finite.

#### D. CONCLUSIONS

We have obtained more rapidly convergent infinite series expressions for the near field pressures and the radiation impedances of circular pistons in an infinite phased array. Numerical results have been obtained for a limited number of cases, and these cases indicate:

1) A single-term approximation  $P_1$ , see Eq. (24), is sufficient to represent the pressure if the distance from the array  $kz$  is larger than 1 or if the array consists of small ( $ka \ll 1$ ) pistons close together.

2) A two-term approximation  $P_2$ , see Eq. (27), gives a rough estimate of the pressure when  $\phi_0 = 0^\circ$ ,  $\theta_0 > 0^\circ$ ,  $kd_1 < \pi$ , and  $kd_2 \leq kd_1$ ; in particular an approximate location, see Eq. (29), and value, see Eq. (31), of the maximum near field pressure can be obtained, and some gross features of the pressure distribution can be predicted.

3) For  $\theta_0 = 0^\circ$  the pressure distribution is relatively smooth, but as  $\theta_0$  increases, the pressure distribution becomes

more undulatory, and the maximum pressure increases.

4) If we keep the piston radius constant and increase the spacing between pistons, the pressure distribution becomes more undulatory.

5) If we keep the ratio of the piston areas to the baffle area constant (sometimes called the "packing factor"), then larger pistons further apart have a larger maximum pressure and a more undulatory pressure distribution than smaller pistons closer together.

6) The near field pressure magnitude and the radiation resistance increase without bounds as  $\theta_o \rightarrow 90^\circ$ , while the radiation reactance remains finite for  $kd_1 < \pi$  and  $kd_2 < \pi$ .

7) The radiation impedance of a piston in the infinite array agrees well with the average radiation impedance of a piston in a large finite array, except near  $\theta_o = 90^\circ$ .

(This Page Intentionally Left Blank)

## REFERENCES

- 1 H. Stenzel and O. Brosze, Leitfaden zur Berechnung von Schallvorgängen (Springer Verlag, Berlin, 1958), 2nd ed., Ch. 4.
- 2 C. H. Sherman and D.F. Kass, U.S.N. Underwater Sound Lab. rept. No. 495 (1961); AD 252964.
- 3 D.T. Porter, U.S.N. Underwater Sound Lab. rept. No. 557 (1962); AD 285963.
- 4 C.H. Sherman, J. Acoust. Soc. Am. 35, 1409-1412 (1963).
- 5 J.E. Greenspon and C.H. Sherman, J. Acoust. Soc. Am. 36, 149-153 (1964).
- 6 A. Freedman, Admiralty Underwater Weapons Establ., Portland, England; tech. note 139/64 (1964); AD 441167.
- 7 N.T. Chin, U.S.N. Underwater Sound Lab. rept. No. 634 (1965).
- 8 V. Mangulis, J. Acoust. Soc. Am 38, 78-85 (1965).
- 9 N.T. Chin, U.S.N. Underwater Sound Lab. rept. No. 681 (1965).
- 10 V. Mangulis, IEEE Trans. Sonics & Ultrasonics (to be published in the July 1966 issue).
- 11 P.M. Morse, Vibration and Sound (McGraw-Hill Book Co., Inc. New York, 1948), p. 327.
- 12 Reference 1, p. 75.
- 13 B. van der Pol and H. Bremmer, Operational Calculus (Cambridge University Press, London, 1955), p. 358.



- 14 Ibid., p. 102
- 15 P.M. Morse and H. Feshbach, Methods of Theoretical Physics  
(McGraw-Hill Book Co., Inc., New York, 1953), p. 466.
- 16 G.N. Watson, Theory of Bessel Functions (Cambridge University  
Press, London, 1958), 2nd ed., p. 359.
- 17 Ibid., p. 132.
- 18 S. Edelberg and A.A. Oliner, IRE Trans. Ant. & Prop. AP-8,  
286-297 (1960).
- 19 R.L. Pritchard, J. Acoust. Am. 32, 730-737 (1960).
- 20 V. Mangulis, J. Acoust. Soc. Am. 34, 1558-1563 (1962).
- 21 C.J. Bouwkamp, Philips Research Reports 1, 251-277 (1946).

TABLE I

Comparison of  $|P_2|_{\max}$  and the actual  
maximum of  $|P|$ .

$kd_1$	$kd_2$	$ka$	$\theta_o$	$ P_2 _{\max}$	Maximum $ P $
3	3	1	$60^\circ$	1.19	1.18
3	3	1	$80^\circ$	2.74	2.55
2.5	2.5	1	$60^\circ$	1.39	1.26
2	2	1	$60^\circ$	1.95	1.64
3	3	1.5	$60^\circ$	2.67	2.04
3	3	0.5	$60^\circ$	0.30	0.47
3	2	1	$60^\circ$	1.78	1.59

$\theta_o = 0^\circ$  for all cases

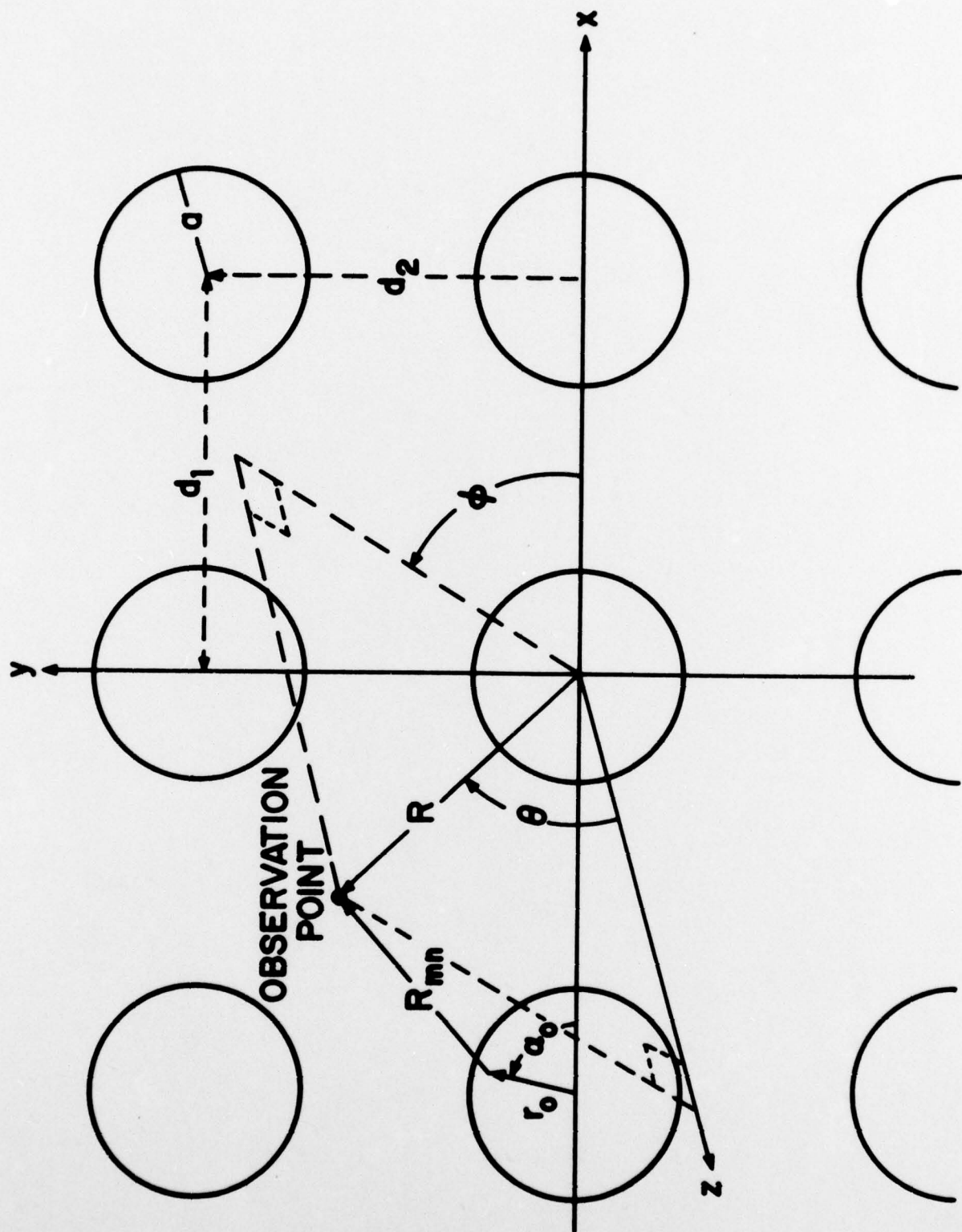
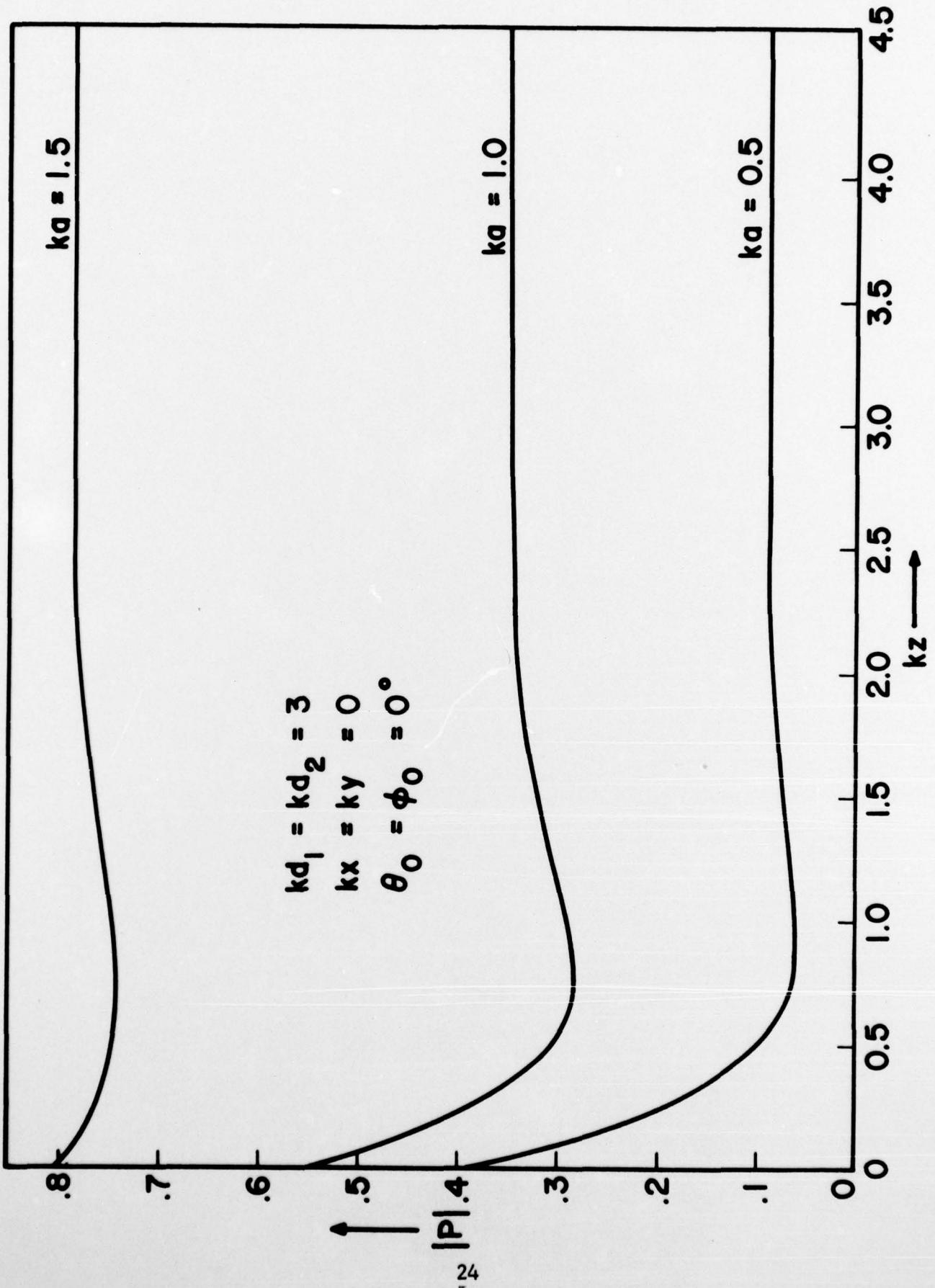
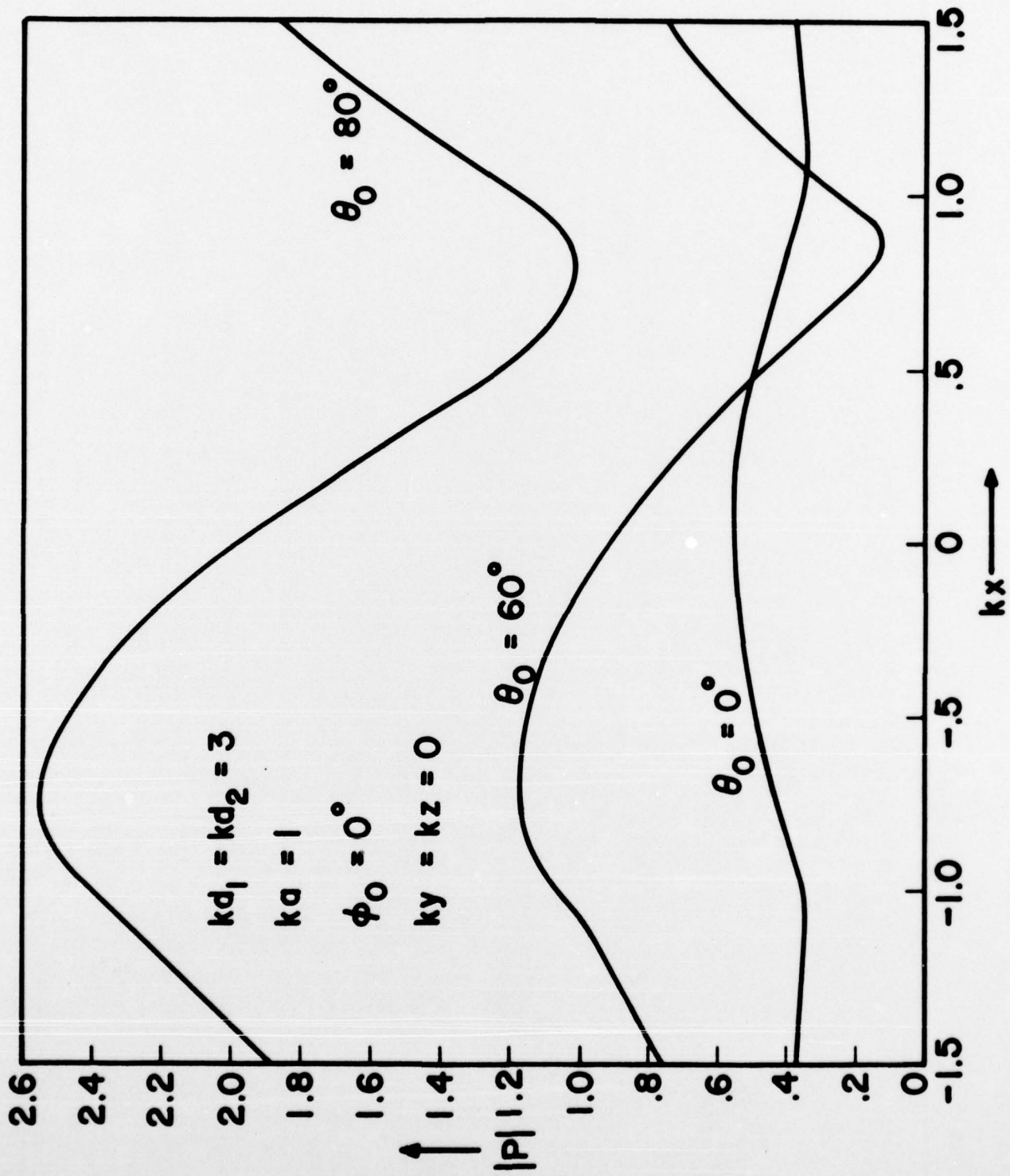
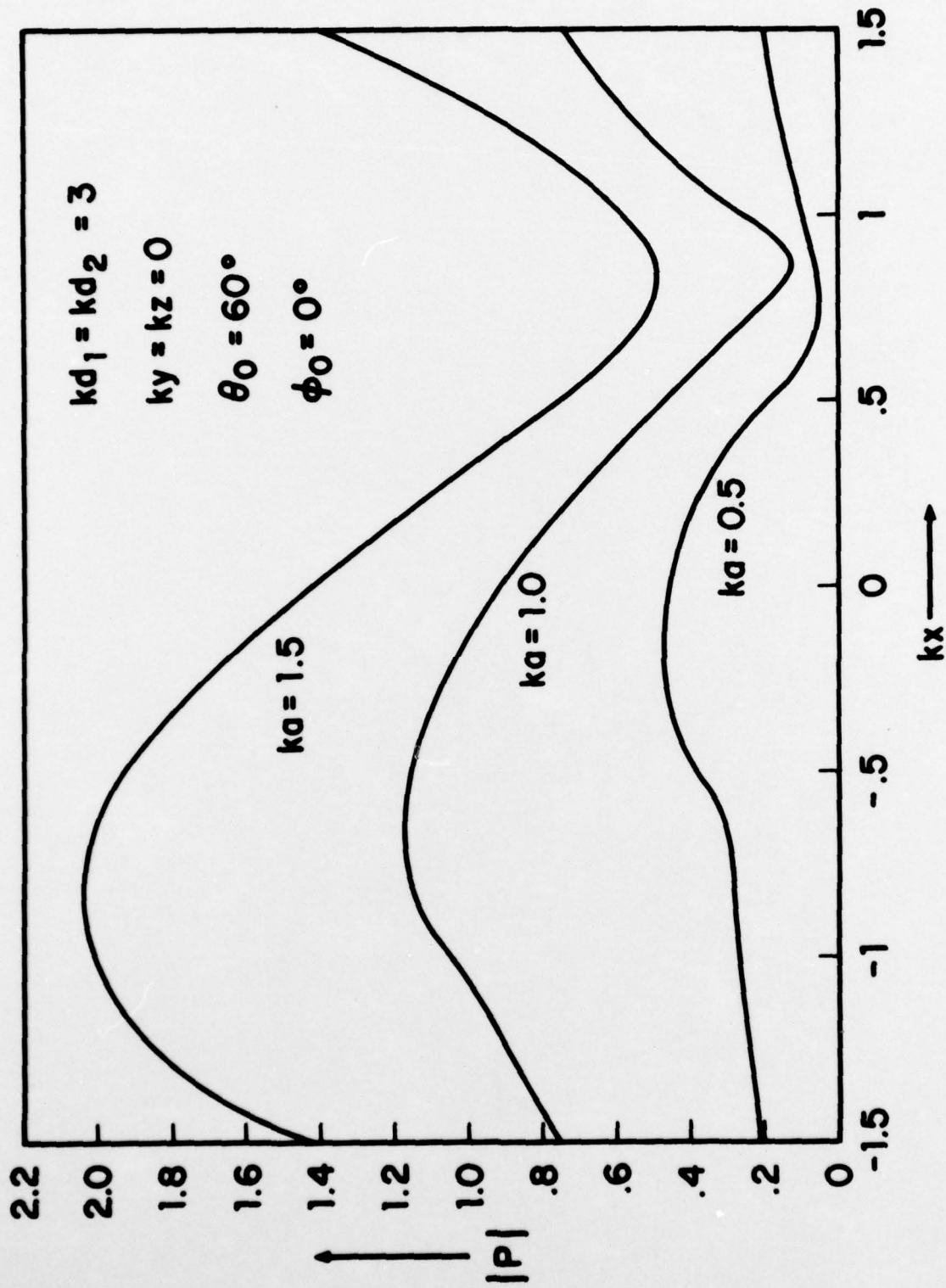


FIGURE 1. PART OF THE INFINITE ARRAY

FIGURE 2.  $|P|$  vs.  $kz$  FOR SEVERAL  $ka$ .



FIGURE 3.  $|P|$  vs.  $kx$  FOR SEVERAL  $\theta_0$

FIGURE 4.  $|P|$  vs.  $kx$  FOR SEVERAL  $ka$

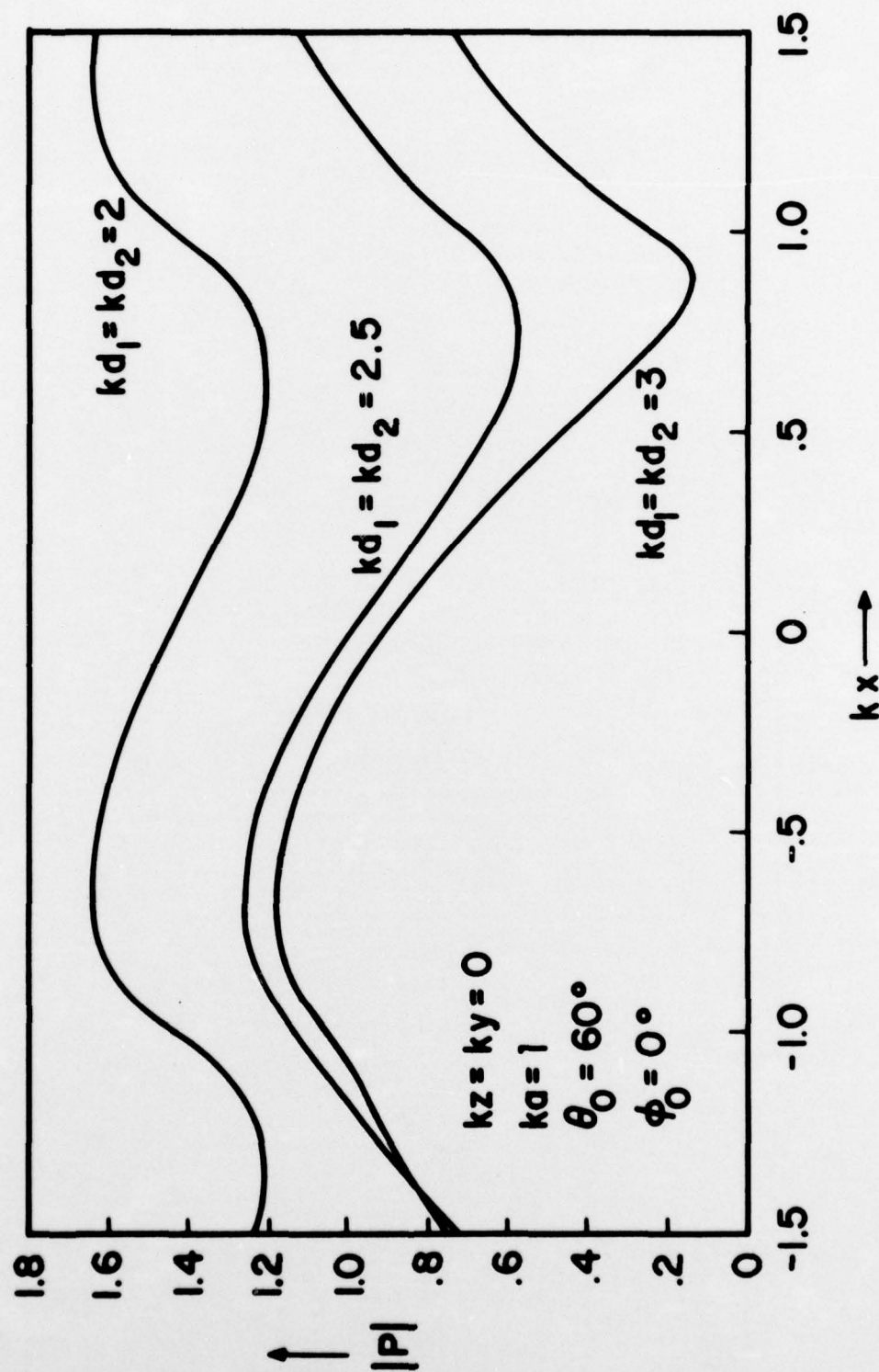


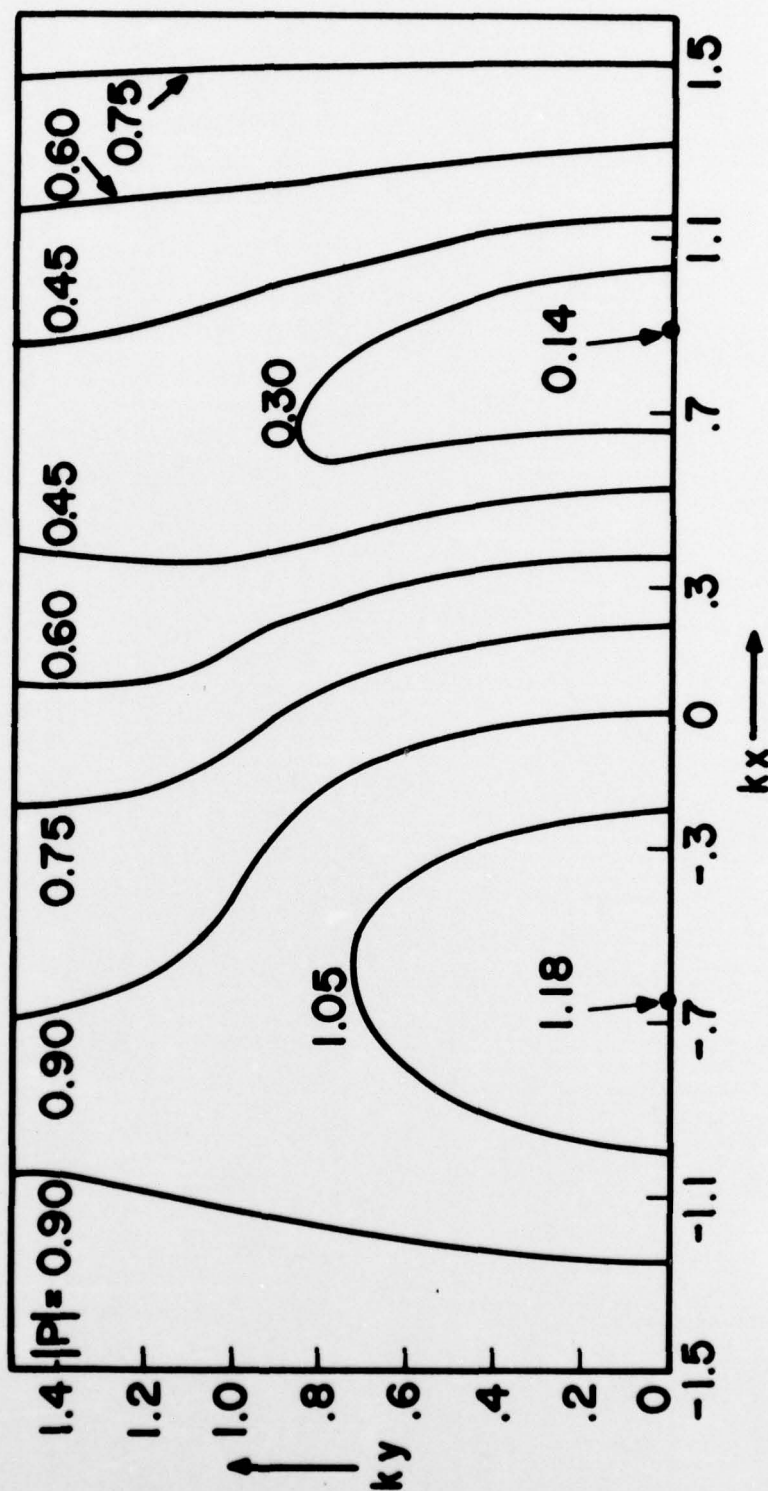
FIGURE 5.  $|P|$  vs.  $kx$  FOR SEVERAL  $kd_1 = kd_2$

$$kd_1 = kd_2 = 3$$

$$ka = 1$$

$$\phi_0 = 0^\circ$$

$$\theta_0 = 60^\circ$$

FIGURE 6. PRESSURE CONTOURS IN THE PLANE  $z = 0$

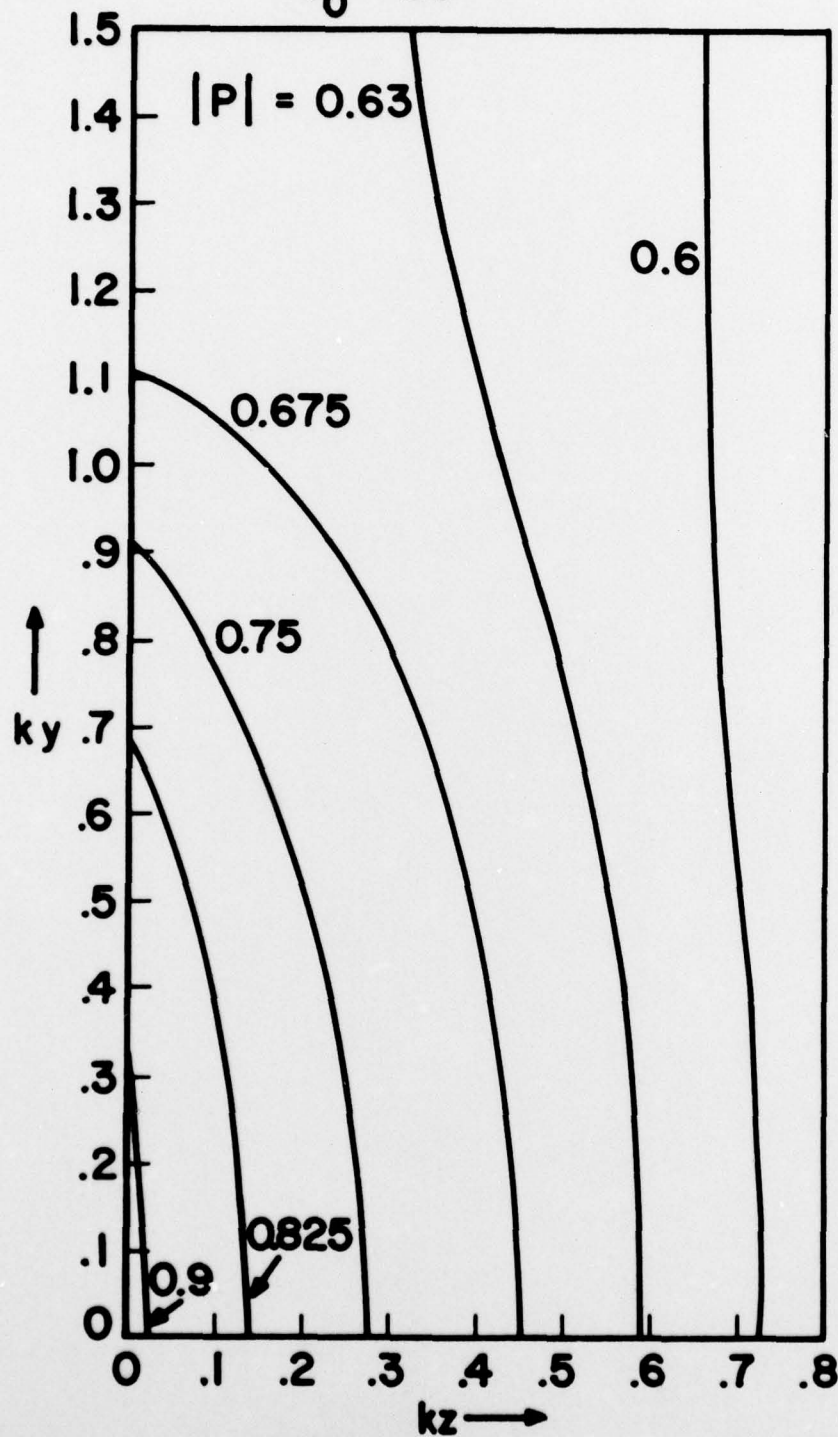


$$kd_1 = kd_2 = 3$$

$$ka = 1$$

$$\phi_0 = 0^\circ$$

$$\theta_0 = 60^\circ$$

FIGURE 7. PRESSURE CONTOURS IN THE PLANE  $x = 0$

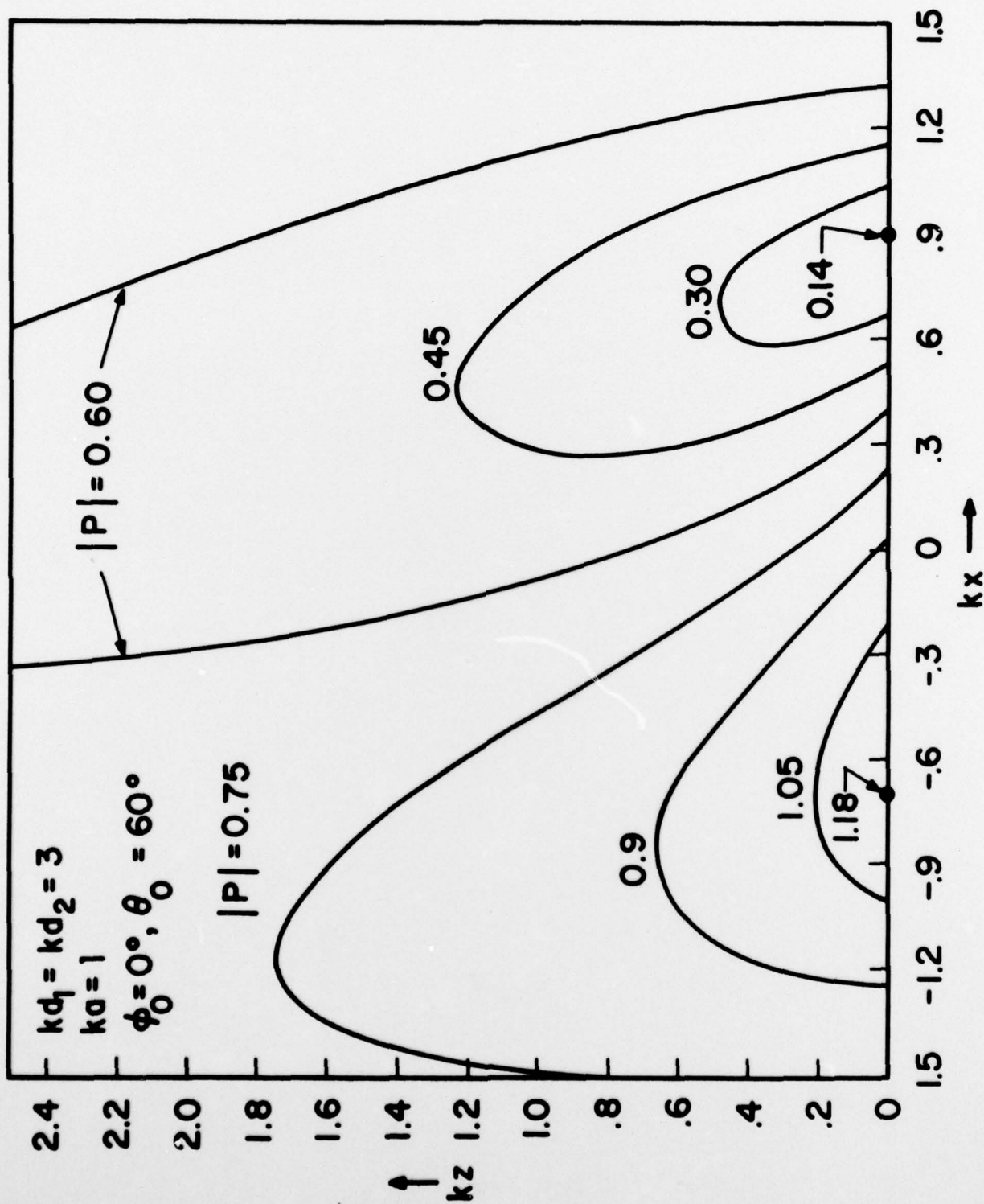


FIGURE 8. PRESSURE CONTOURS IN THE PLANE  $y = 0$

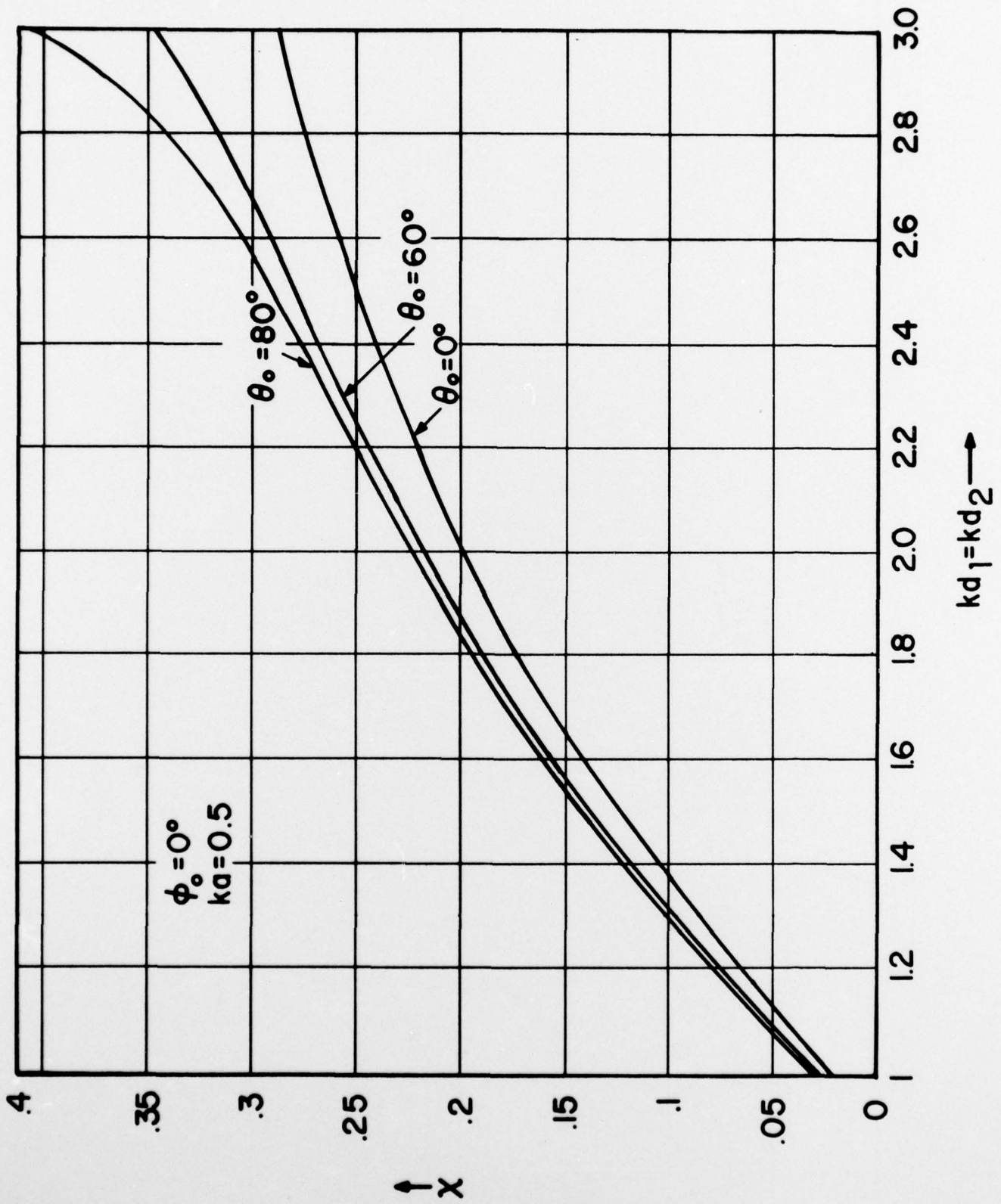
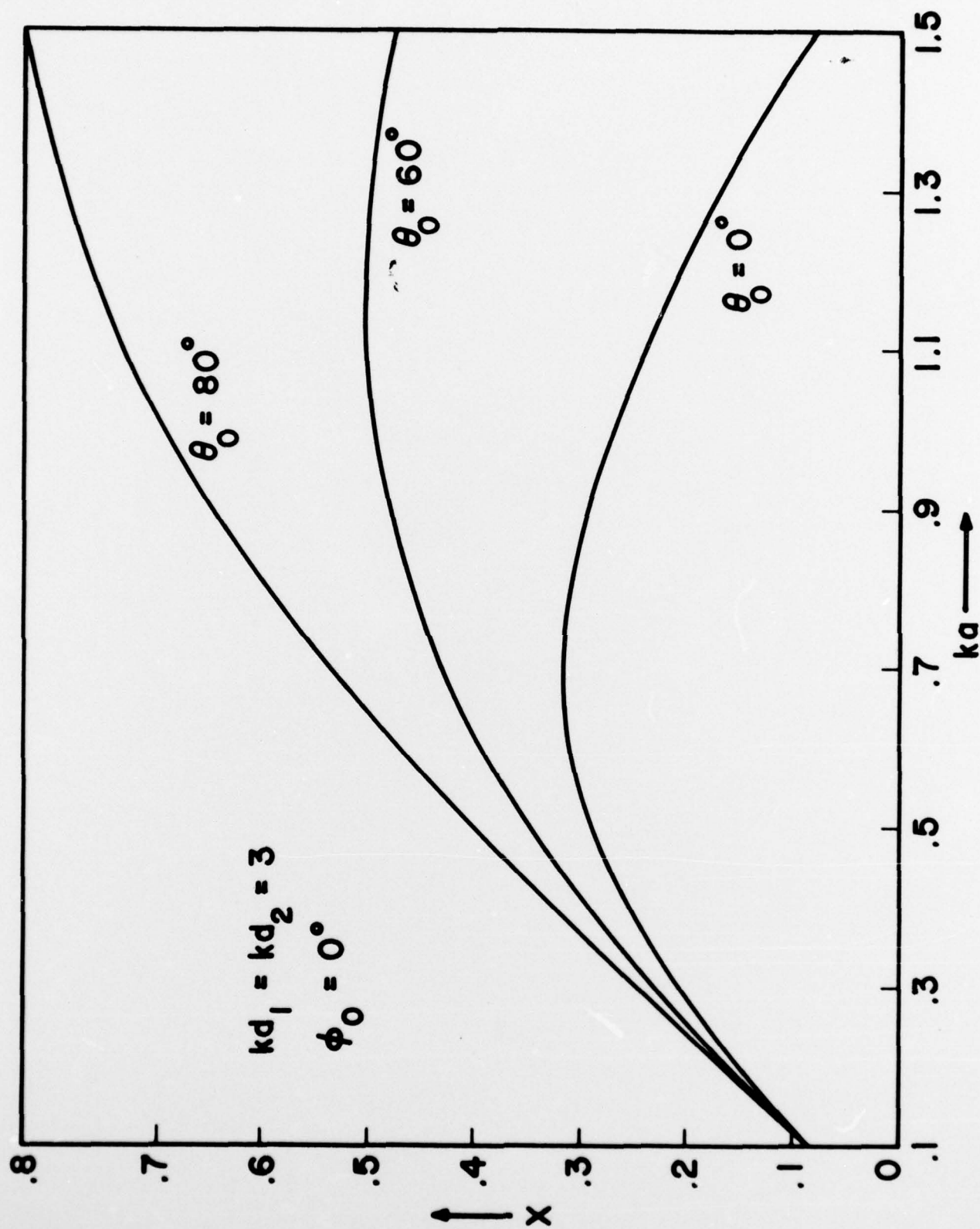
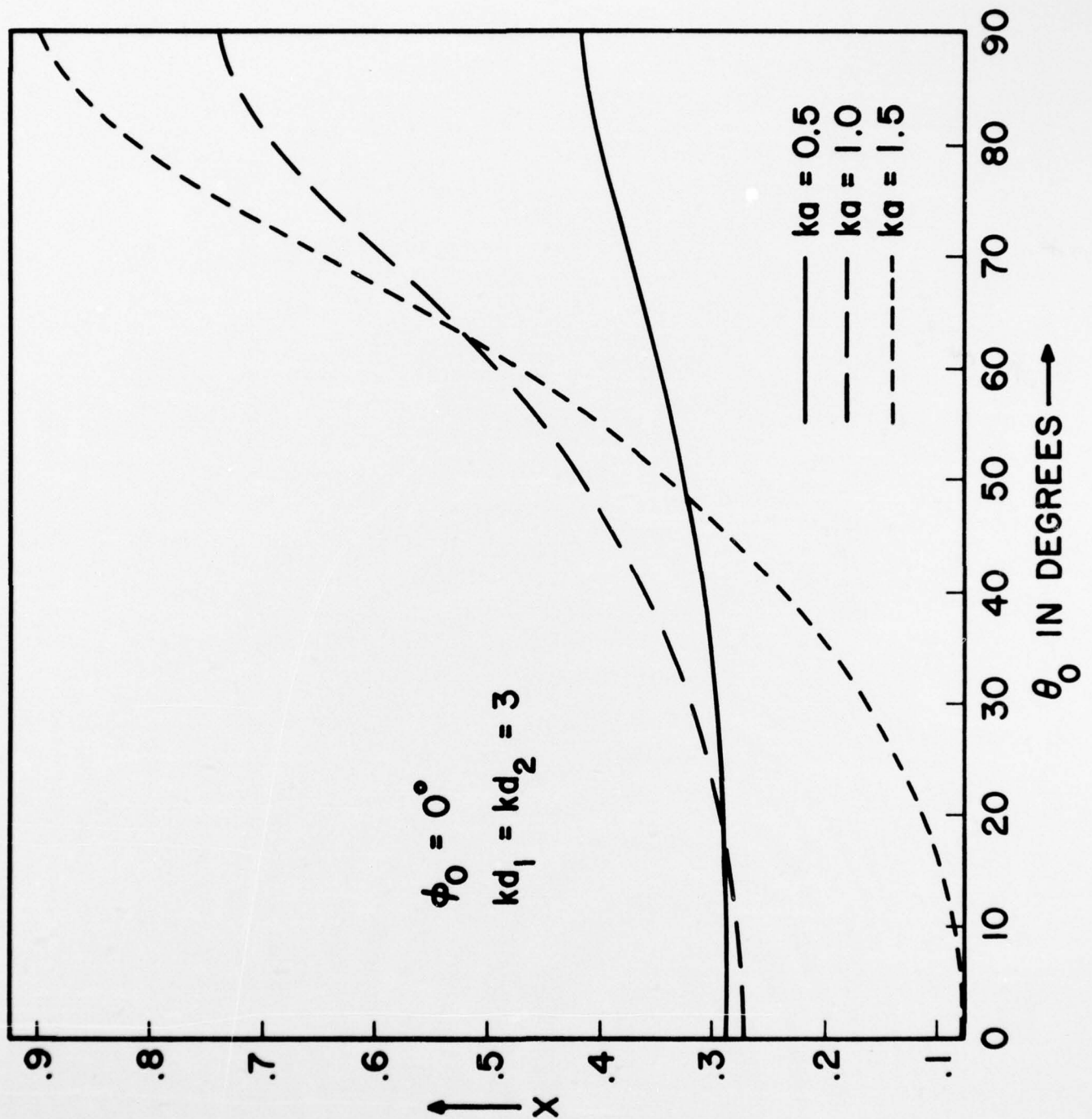
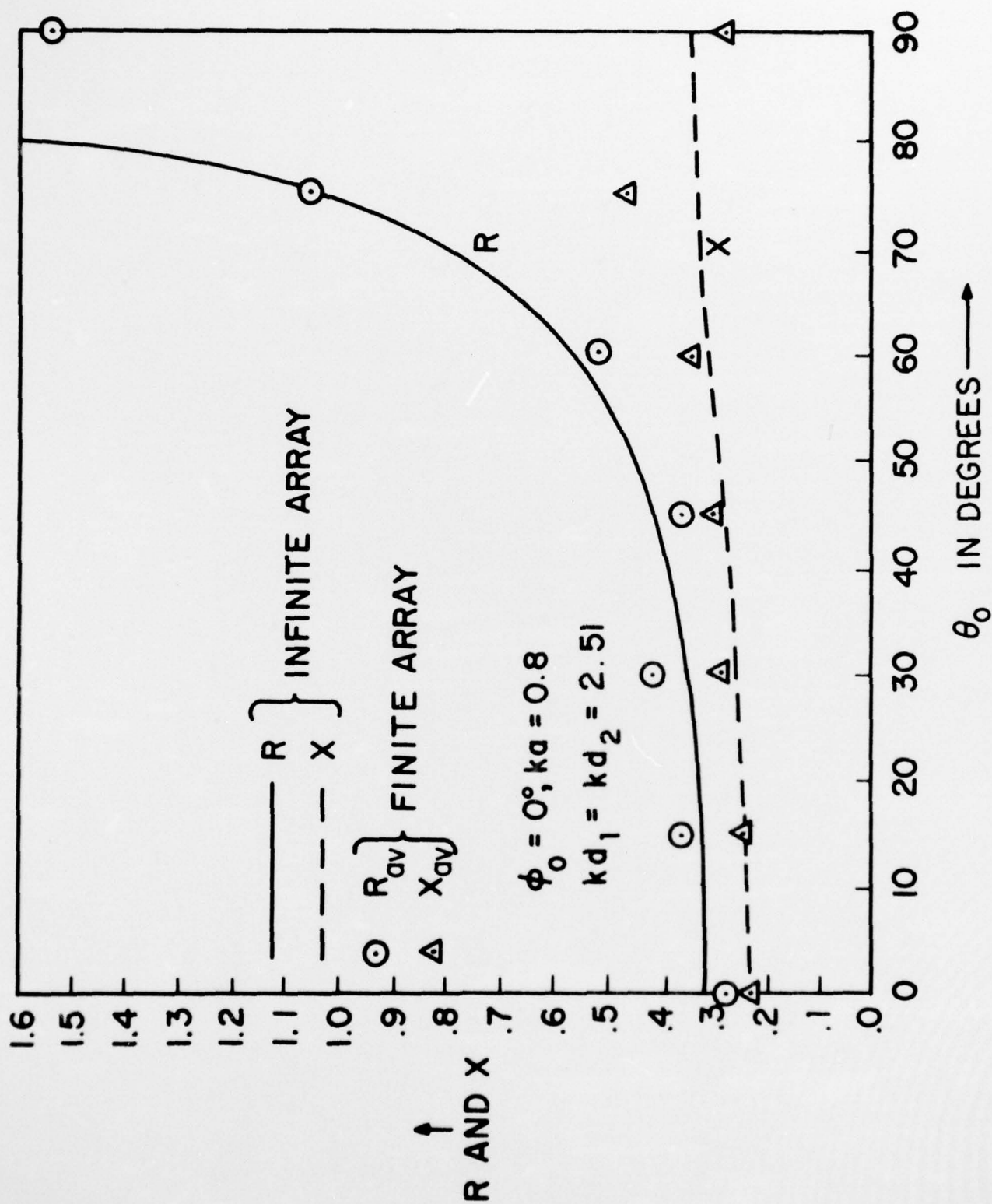


FIGURE 9.  $X$  vs.  $kd_1 = kd_2$  FOR SEVERAL  $\theta_0$

FIGURE 10.  $X$  vs.  $ka$  FOR SEVERAL  $\theta_0$



FIGURE 11.  $X$  vs.  $\theta_0$  FOR SEVERAL  $ka$

FIGURE 12. RADIATION IMPEDANCE vs.  $\theta_0$ , FINITE AND INFINITE ARRAYS